forests

MDPI

Article

Maximum Rooting Depth of *Pinus thunbergii* Parl. Estimated with Depth at the Center Point of Rotation in a Tree-Pulling Experiment in a Coastal Forest in Japan

Chikage Todo [1,2,*], Keitaro Yamase [1], Hidetoshi Ikeno [3], Toko Tanikawa [4], Mizue Ohashi [5] and Yasuhiro Hirano [2]

[1] Hyogo Prefectural Technology Center for Agriculture, Forestry and Fisheries, Shiso 671-2515, Japan
[2] Graduate School of Environmental Studies, Nagoya University, Nagoya 464-8601, Japan
[3] Faculty of Informatics, The University of Fukuchiyama, Fukuchiyama 620-0886, Japan
[4] Graduate School of Bioagricultural Sciences, Nagoya University, Nagoya 464-8601, Japan
[5] School of Human Science and Environment, University of Hyogo, Himeji 670-0092, Japan
* Correspondence: chikage_toudou@pref.hyogo.lg.jp

Abstract: Tree resistance to uprooting can be estimated as the critical turning moment in tree-pulling experiments. The depth at the center point of rotation (Dcp) in tree-pulling experiments is measured as an indicator of below-ground traits and is related to this critical turning moment. However, few researchers have investigated the relationship between the Dcp and maximum root depth. Our objective in this study was to clarify whether the Dcp in tree-pulling experiments can be estimated as the maximum root depth of *Pinus thunbergii* Parl. in sandy soils. We also estimated which position of displacement of the center of rotation (Cp) can be applied as the Dcp. We conducted tree-pulling experiments, and compared the Dcp obtained from images with the measured maximum root depth. We found significant positive correlations between the Dcp and maximum root depth. The Cp displacement concentrated immediately below the stem when the maximum critical turning moment was reached. This position should be measured as the Dcp, which is related to the maximum root depth. We found that the Dcp can serve as a parameter, preventing the need for uprooting, when tree-pulling experiments are performed to obtain an important below-ground trait for understanding the critical turning moment.

Keywords: root depth; center point of rotation; root system; tap root; tree-pulling experiment; uprooting

Citation: Todo, C.; Yamase, K.; Ikeno, H.; Tanikawa, T.; Ohashi, M.; Hirano, Y. Maximum Rooting Depth of *Pinus thunbergii* Parl. Estimated with Depth at the Center Point of Rotation in a Tree-Pulling Experiment in a Coastal Forest in Japan. *Forests* **2022**, *13*, 1506. https://doi.org/10.3390/f13091506

Academic Editor: Brian Kane

Received: 12 August 2022
Accepted: 11 September 2022
Published: 16 September 2022

1. Introduction

Coastal forests play an important role in preventing damage from strong salty winds caused by the sea and tsunamis [1,2]. Most coastal areas in Japan have been planted with *Pinus thunbergii* Parl., which has been resistant to salt and wind for the past several hundred years [3,4]. In 2011, the Great East Japan Earthquake triggered a tsunami that severely damaged the coastal *P. thunbergii* forests, which caused uprooting and stem breakage in *P. thunbergii* in several coastal forests [5]. Although *P. thunbergii* originally had deep tap roots [6], the uprooted trees in the damaged coastal forests had plate root systems because of the shallower groundwater table [5]. In previous studies, we found that the contrasting systems of the plate or tap roots of *P. thunbergii* under different groundwater depths in a coastal forest have different levels of resistance against tsunami using tree-pulling experiments and the subsequent harvesting and measurement of root systems [7,8].

The resistance of trees to uprooting caused by strong winds or tsunamis can be estimated as the critical turning moment [7,9–15], which is defined as the force × length of the lever arm [16]. To evaluate critical turning moments in Japan, tree-pulling experiments have often been conducted without uprooting because of legal regulations regarding

forest preservation [7,17–19]. The above-ground traits of trees that are directly affected by wind and tsunamis, namely stem diameter at breast height (DBH) and stem volume related parameter (height (H) × DBH^2), have a strong relationship with the critical turning moment and are thus suitable predictors of tree resistance [7,13,14,20]. In the case of wind, the dimensions and shape of the crown are appropriate predictors of tree resistance [21]. The below-ground traits, such as the root system structure, also affect the critical turning moment [9–14,16,20,22–28]. In a case study on the effect of below-ground traits, in the 17 years after thinning management, *Cryptomeria japonica* (L. f.) D. Don. trees exhibited significantly higher critical turning moments than unthinned trees when trees with the same stem volumes were compared [17]. The reason for the higher critical turning moment in the thinned trees was the increased horizontal radius of the root-soil plate (RSP), which promoted horizontal root growth [17]. Cucchi et al. [13] also reported that the critical turning moments of trees at the border of a stand were higher than those of trees from inside the stand, probably because of their larger RSP volume. In such cases, the above-ground traits are not always predictors of tree resistance. In addition to above-ground traits, below-ground traits, such as root system type (tap or plate root system), horizontal spread, and rooting depth, can contribute to the critical turning moment [13,16,17]. Thus, differences in belowground traits should also be evaluated to determine the factors contributing to the critical turning moment and tree uprooting mechanism.

To measure below-ground traits, uprooting and digging of root systems have been adopted in tree-pulling experiments [4,29,30]. Such measurements of below-ground traits are time-consuming, labor-intensive, and impractical for repeated measurements [8,31,32]. The maximum root depth is particularly difficult to directly measure [8] and depends on tree species, soil conditions, presence of bedrock, and groundwater level [25,29,30,33]. The maximum critical turning moment is strongly affected by the maximum depth of the tap roots in *Pinus* species [28,34]. Deep rooting at the same stem mass as *Picea sitchensis* (Bong.) Carr. increases the critical turning moment by 10%–15% compared with shallow rooting [16]. In a tree anchorage simulation, a tap root system exhibited a larger critical turning moment than the plate or herringbone root systems [35]. These data indicated that maximum root depth is closely related to resistance to uprooting. Thus, evaluating the maximum root depth is important for understanding the critical turning moments and tree uprooting mechanisms [16,28,34,35]. Therefore, if the maximum root depth can be estimated using simple measurements during tree-pulling experiments, the contribution of below-ground traits to uprooting resistance in various tree species can be further understood.

As a candidate method for simple measurements during tree-pulling experiments, the depth at the center point of rotation (Dcp) has been proposed as an indicator of the maximum depth of the RSP [7,17–19,36–38]. Dcp is the depth from the ground surface to the position at which the displacement of the center point of rotation (Cp) converges (Figure 1) [7,17,19,38]. Dcp was originally devised to estimate root system stability in a standing tree that was used as an anchor for cable yarding in timber logging, and was calculated against the lateral loads of wire ropes [36]. The advantages of this indicator are twofold: first, it can be relatively quickly calculated based on video images of the test tree from the beginning of the tree-pulling experiment until immediately after recording the maximum critical turning moment [7,17,36]; second, a test tree does not need to be uprooted [7,17,36]. As the tree starts to uproot along the boundary between the outside soil and the RSP in response to lateral forces [6], the assumptions are that (i) the tree rotates at a point on the vertical line through the stem center within a relatively small range of inclination (Figure 1a) and (ii) both the lateral movement of the tree toward the load and the bending range of the stem around the root trunk are negligible. In this study, we set measuring points P1 and P2 on a vertical straight line through the stem center of a test tree at different heights from the ground surface without any lateral forces. After loading the lateral forces, we measured the new positions of P1 (P1′) and P2 (P2′). We measured the point where the lines passing through P1 and P2 and through P1′ and P2′ intersect as the Cp, and the depth from the ground surface to Cp as the Dcp (Figure 1a, [36]).

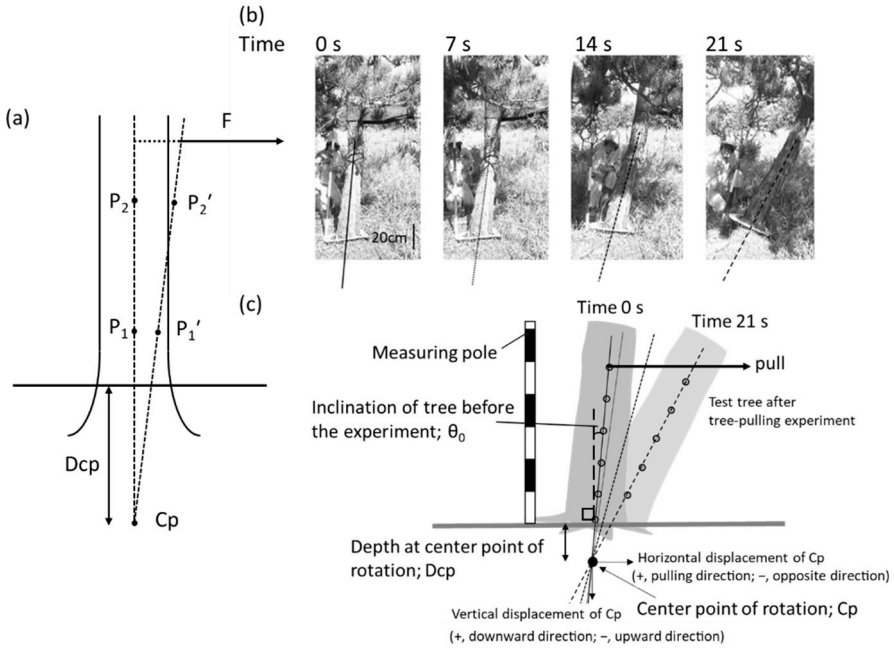

Figure 1. Method of measuring center point of rotation (Cp) and depth at center point of rotation (Dcp) during tree-pulling experiment. (**a**) General scheme (modified from Morioka [36]), (**b**) positions of straight vertical lines on stem surface every 7 s, and (**c**) measurement details.

Morioka [36] showed that the Dcp of *C. japonica* trees with a DBH of 6–21 cm was 13–52 cm, and concluded that the outer range reflects the depth of the RSP. During a tree-pulling experiment, Nonoda et al. [18] demonstrated that *Chamaecyparis obtusa* (Siebold et Zucc.) Endl. rotated at the center point just below the stem. Kamimura et al. [39] reported that the horizontal displacement of *C. obtusa* stems after loading with lateral forces was only a few millimeters and was thus negligible. Because the maximum root depth increases with increasing RSP depth [10], the maximum root depth can be assumed to be related to the Dcp.

The results of tree-pulling experiments have shown that Dcp is positively related to the maximum critical turning moment [7,17,18,38]. The Dcp in *P. thunbergii* trees was deeper in a land-side plot, having a relatively higher maximum critical turning moment, than in a sea-side plot [7]. However, researchers have not yet examined the relationship between the Dcp and maximum root depth of the target tree in a field. To understand the uprooting mechanisms related to the maximum root depth, the accuracy of the relationship must be determined.

The Cp position can change with increasing load during tree-pulling experiments, because the respective positions of the rotation axis depend on the soil properties and root structure [40]. In tree-pulling experiments on *C. japonica* and *C. obtusa*, Cp was concentrated at a single point just below the stem [18,36]. In contrast, Coutts [9] reported that the Cp of *P. sitchensis* during uprooting is located at the upper edge of the RSP on the leeward side. The displacement of Cp must be determined to indicate the measured position of Dcp. Therefore, the displacement of Cp should be monitored during tree-pulling experiments to clarify the discrepancy in the position of Cp at the time of the maximum critical turning moment, that is, Dcp. This will support the use of Dcp at the right position as an indicator of the maximum root depth in tree-pulling experiments.

In this study, we targeted a temperate *P. thunbergii* forest growing in sandy soil in coastal areas prone to tsunamis and wind damage. The objectives of this study were to clarify (i) whether Dcp in tree-pulling experiments is related to the maximum root depth and (ii) which position of displacement of Cp can be applied as Dcp. If the maximum root depth is estimated from Dcp, the below-ground traits of the target tree can be simply

described in tree-pulling experiments, which can lead to further understanding of its contribution to uprooting processes.

2. Materials and Methods

2.1. Study Site

The study site was located in a coastal *P. thunbergii* forest stretching 8 km west of the Atsumi Peninsula in Tahara City, Japan [7,8,41,42]. In the event of a major earthquake in the region, tsunami wave heights of up to 4 m were predicted [43]. Most trees in the forest were replanted in the 1960s after being heavily damaged by Typhoon Vera in 1959 [44]; management has been performed only for the treatment of pine wilt disease to remove dead trees [45]. The soil was sandy and classified as Regosol [46]. From 1981 to 2010, the mean annual temperature was 16 °C and the mean annual precipitation was 1603 mm [47]. At the nearest weather station, Irago (34°37′ N, 137°05′ E), the 30-year (1981–2010) annual mean wind speed was 3.8 m s^{-1} and the daily maximum wind speed was 26.2 m s^{-1} [38]. The groundwater level was almost constant from the shoreline inland [41]. However, the depth of the groundwater level from the ground surface deepened inland as elevation increased (Table S1).

Within the continuous *P. thunbergii* forest, the stands had different tree growths, which was due to the different depths of the groundwater table (Tables 1 and S1) [7,8,41,42]. Therefore, we divided the stands into three sections, and surveyed representative sites as plots (Figure S1 [7,8,41,42]). Plot A was located 188–199 m from the shoreline [41,42]; plot B was also located close to the shoreline (150–270 m). Plot C was further from the shoreline (620–740 m [7]; Figure S1). The mean age of the *P. thunbergii* in the three plots was 45 years. The *P. thunbergii* stand density was lowest in plot A (100–200 individuals ha^{-1}), and mid-range in plot B (200–400 individuals ha^{-1}), and highest in plot C (400–1000 individuals ha^{-1}). Table S1 summarizes the other characteristics, such as soil water content and understory species among the plot. We established the locations where we dug the test trees within the plots. The areas where the *P. thunbergii* trees were dug out were 400 × 15 m for plot A, 120 × 180 m for plot B, and 170 × 120 m for plot C.

Table 1. Above- and below-ground traits of ten *Pinus thunbergii* trees.

Plot	Tree No.	Age (Years)	θ_0 (Degrees)	H (m)	DBH (cm)	H × DBH^2 (m^3)	Critical Turning Moment (kN m)	Maximum Root Depth (cm)	Dcp (cm)	RSPRadius (cm)	RSP Radius/ Dcp
Plot A	1	50 [a]	–5.1	11.4 [a]	18.5 [a]	0.39	33.4	126.0 [a]	29.7	90.7	3.1
	2	45 [a]	–0.09	10.8 [b]	19.5 [b]	0.41	25.5 [a]	106.0 [a]	23.3	61.9	2.7
	3	40	–1.4	9.3 [b]	15.9 [b]	0.23	12.7	44.0	17.0	67.7	4.0
	4	51	–3.1	10.1 [b]	16.4 [b]	0.27	16.4	86.0	18.0	58.8	3.3
	Mean	46.5	–2.4	10.4	17.6	0.33	22.1	90.5	22.0	69.8	3.2
Plot B	1	36 [c]	7.5	7.4 [c]	17.0 [c]	0.21 [c]	25.7 [c]	75.0 [c]	12.9 [c]	73.4 [c]	5.7
	2	39 [c]	16.2	7.1 [c]	22.8 [c]	0.37 [c]	41.2 [c]	57.5 [c]	3.1 [c]	104.4 [c]	34.0
	3	44 [c]	9.5	4.4 [c]	16.9 [c]	0.13 [c]	17.8 [c]	35.0 [c]	5.2 [c]	50.8 [c]	9.8
	Mean	39.7	11.1	6.3	18.9	0.24	28.2	55.8	7.1	76.2	16.5
Plot C	1	32 [c]	–11.2	8.9 [c]	18.7 [c]	0.31 [c]	48.3 [c]	175.0 [c]	24.7 [c]	58.4 [c]	2.4
	2	51 [c]	3.7	13.8 [c]	18.3 [c]	0.46 [c]	50.4 [c]	240.0 [c]	34.7 [c]	43.3 [c]	1.2
	3	58 [c]	–10.8	11.7 [c]	23.7 [c]	0.66 [c]	84.3 [c]	222.0 [c]	41.3 [c]	99.9 [c]	2.4
	Mean	47.0	–6.1	11.5	20.2	0.48	61.0	212.0	33.6	67.2	2.0

DBH: stem diameter at breast height; Dcp: depth at center point of rotation. H: stem height; RSP: root soil plate; θ_0: inclination of the tree before the experiment (inclination from the ground to the vertical line, with the direction of the pull considered +). [a] Data from Todo et al. [42]. [b] Data from Tanaka et al. [41]. [c] Data from Todo et al. [7] and Hirano et al. [8].

2.2. Tree-Pulling Experiments and Root System Excavation of P. thunbergii

We selected ten *P. thunbergii* trees from the three plots to examine the relationships between the maximum critical turning moment, Dcp, and maximum root depth (Table 1).

We selected only 10 average trees because complete excavation was legally limited in Japan for forest protection. The selected trees grew 188–734 m from the shoreline, and the mean DBH was 18.8 cm (Table 1). The mean H tended to be larger in plots A and C than in plot B (Table 1). The inclination of the trees (θ_0, Figure 1c, Table 1), where we set the line perpendicular to the ground to 0° and the direction of pull in the experiment was positive, ranged from –11.2° to 16.2°. We observed the highest inclination in Plot B.

We conducted tree-pulling experiments following the method described by Todo et al. [7,42]. Briefly, we connected test trees with polyester belt slings (safe load 6.3 t) to a 10 mm diameter wire rope at a height of 1.0 m above the ground (1.5 m for only one tree in plot C3), and the trees were pulled parallel to the ground by an excavator (Figure S2). We recorded load data at 0.1 s intervals via a bridge unit (DBU-120A, Kyowa Denshi Kogyo Co., Ltd., Tokyo, Japan) with a load cell (maximum load of 50 kN, LT-50KNG56 Nikkei Densoku Co., Tokyo, Japan) connected between the belt sling and wire rope. We measured the load before the wire rope began pulling the tree and reached a maximum value, that is, the critical turning moment. Subsequently, the load began to decrease, at which point we stopped the measurement (Figure S3); therefore, we used none of the trees were uprooted in this study. We calculated the critical turning moment (M) using Equation (1) [7,42].

$$M = F \times h \times \cos\theta_0 \quad (1)$$

where F (kN) is the maximum applied force, h (m) is the attachment height of the pulling sling, and θ_0 (°) is the angle of the vertically inclined trees.

In the tree-pulling experiments, cracks appeared on the ground surface on the side opposite of the pulling force. Owing to logging restrictions at the study site, we could not measure the RSP by complete uprooting. We defined the RSP radius as the average distance from the arcs at the edges of the formed RSP (i.e., cracks) to the center of the stem [7]. We measured ten points of the RSP radius for individual trees [7]. We calculated the ratio of the RSP radius to Dcp (RSP radius/Dcp) as an indicator of the RSP shape.

We measured the maximum depth of the tap root by carefully digging out the entire root system using an air spade (Air Schop, J-LINK Co., Yokohama, Japan) to avoid damaging the roots. The detailed methods were described by Hirano et al. [8]. During excavation, we removed the soil step-by-step to avoid moving the root system, partly fixed with piles, in the soil. The diameter of the tap root at maximum depth was set to 2 cm. We used a tape measure along the root system to determine the maximum root depth.

2.3. Calculation of Dcp and Cp Displacement

We estimated the Dcp and Cp positions in the tree-pulling experiments using the method proposed by Morioka [36] (Figure 1a) and as described in detail by Todo et al. [7]. Briefly, we captured images of the stem during the tree-pulling experiment using a video camera (HDR-CX180, Sony Co., Tokyo, Japan) set perpendicular to the pull direction (Figure S2). We marked six points on the stem surface at vertical intervals of 20 cm from the ground level to a height of 100.0 cm to monitor positional changes [7]. We installed a measuring pole adjacent to the test tree for scaling (Figure 1). We fixed the position of the video camera when capturing the images of each test tree, and we did not use the zoom function.

We tracked the Cp position in 1 s intervals. We also extracted the x and y coordinates of the marks on the tree in 1 s intervals. We created a straight line from all images using the two marks that were clearest and easiest to capture, and we then calculated Cp (Figure 1b). We measured the horizontal displacement (Figure 1c) parallel to the ground surface of each tree as the distance from the start of the tree-pulling experiment, which we defined as 0. We measured the vertical displacement (Figure 1c) at the Cp for each tree as the distance from the ground surface. We thus determined the position of the Cp at the time of the critical turning moment exertion, and we identified the depth of Cp at that time from the ground surface as the Dcp. We measured the length per pixel on a scale. We converted the horizontal and vertical displacements measured in pixels to displacements in centimeters

using the length per pixel. We evaluated the misalignment of Cp (msaCp) toward zero from the start of pulling by the commonly used Euclidean distance using the following formula:

$$\text{msaCp} = \sqrt{(x - x_m)^2 + (y - y_m)^2} \quad (2)$$

where x and y are the horizontal and vertical coordinates of Cp, respectively, at each time point during the pulling experiments; x_m and y_m are the horizontal and vertical coordinates of Cp, respectively, when the critical turning moment is the maximum.

It was important that there be no significant deflection in the stem in order to measure Dcp by connecting the marks on the stem with a line [36]. In this case, we observed no large deflection of the test tree when a video was captured. The wire rope attached during the pulling experiment was approximately 1 m above the ground, and we assumed the stem to be a rigid body. We used open-source software ImageJ version 1.51 [48] for image processing and measurements.

2.4. Data Sets and Statistical Analysis

In the current study, we used data from previous studies by Tanaka et al. [41], Hirano et al. [8], and Todo et al. [7,42] (Table 1). Tanaka et al. [41] and Todo et al. [42] reported the data on DBH and H for each tree in plot A and the data on critical turning moment and maximum root depth for the two trees in plot A (Table 1). Todo et al. [7] reported the data on DBH, H, H $\times$ DBH^2, critical turning moment, and Dcp for each tree in plots B and C (Table 1). Hirano et al. [8] reported the mean maximum root depths in plots B and C. The mean maximum tap root depth was 55.8 $\pm$ 11.6 cm in plot B and 212.3 $\pm$ 19.4 cm in plot C [8]. Plate root systems with long horizontal roots but few tap roots were observed in plot B, which had a shallow groundwater level, whereas tap root systems were observed in plot C, which had a deep groundwater level [8].

In this study, we newly acquired and analyzed the data on the critical turning moment, maximum root depth of the two trees, and Dcp of each tree in plot A; RSP radius and the horizontal and vertical displacements of Cp with time of tree pulling in all plots (Table 1).

We used the Mann–Whitney U test to detect the differences between the horizontal and vertical displacements. We tested the relationships between traits using Spearman's rank correlation coefficient. We performed statistical analyses using R software version 4.0.2 [49] with a significance level set at $p < 0.05$.

3. Results

In all three plots, the horizontal Cp displacement (mean, 3.1 cm) during the tree-pulling experiments was approximately 10% of the vertical displacement (mean, 28.3 cm), and the difference was significant (Figure 2). Cp did not laterally or vertically displace when the maximum value of the critical turning moment was reached (Figure 2), and concentrated at a single point almost directly below the stem (Figure 3a). We set the misalignment of the Cp with the relative time to the duration of reaching the maximum critical turning moment to one, which thus converged to zero; that is, the Cp position reached a single point (Figure 3b). The results showed that the position of Cp did not move with increasing tensile time when the critical turning moment was close to its maximum value compared with just after the start time of the tree-pulling experiment (Figure 3b).

In plot A, the critical turning moment was 12.7–33.4 kN m and the maximum root depth was 44–126 cm (Table 1). Except for one tree, tap root systems developed below 80 cm in plot A. The mean Dcp value tended to be smaller in plot B than in plots A or C (Table 1). The ratio of RSP radius/Dcp tended to be larger (5.0) in plot B than in plots A and C, indicating that the shape of the RSP in plot B tended to be laterally larger than deep (Table 1).

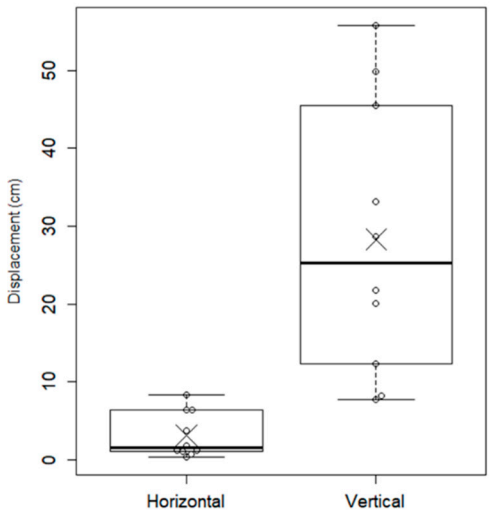

Figure 2. Box-and-whisker plots of the maximum horizontal and vertical displacements from the beginning of the tree-pulling experiment until reaching the maximum critical turning moment in *Pinus thunbergii* trees. The median value is shown as a horizontal black line inside the box; the first and third quartiles are the bottom and top of the box, respectively. Each line vertically extending from the box represents 1.5 times the interquartile distance. The mean is shown as an x mark. Univariate scatter plots show data points of 10 individual trees.

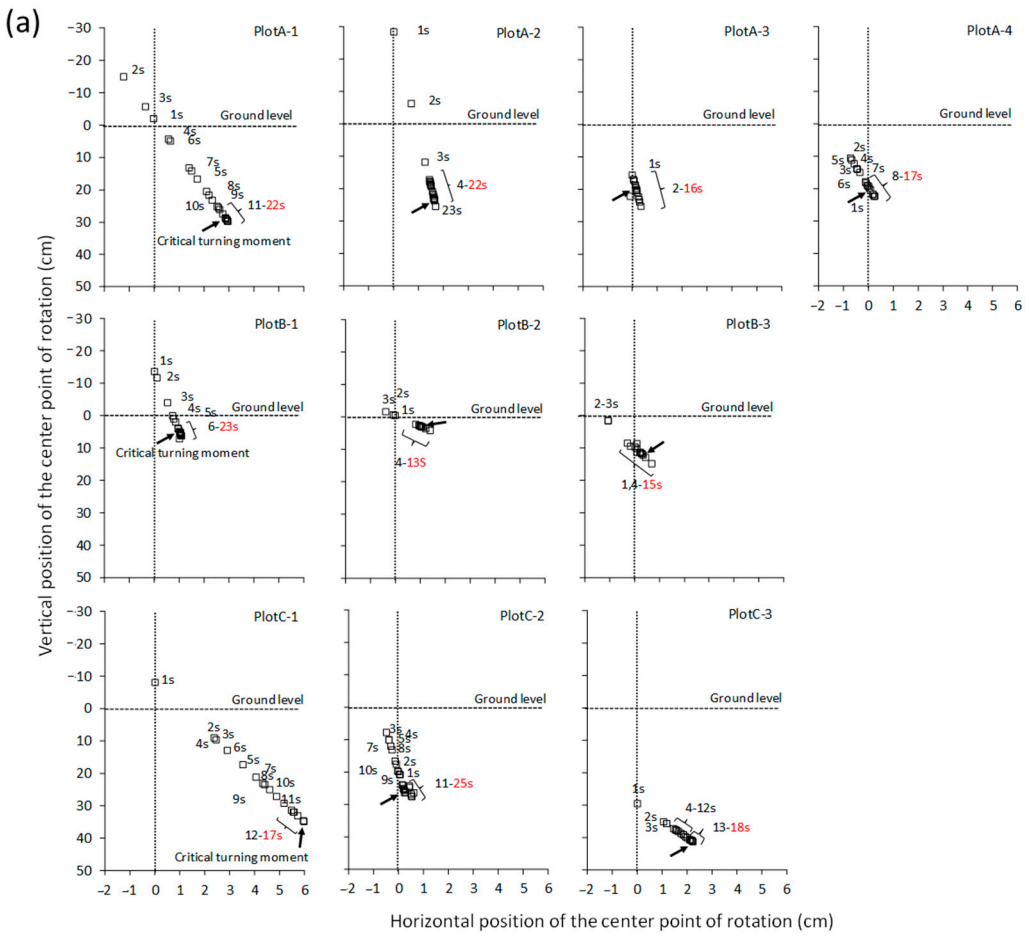

Figure 3. *Cont.*

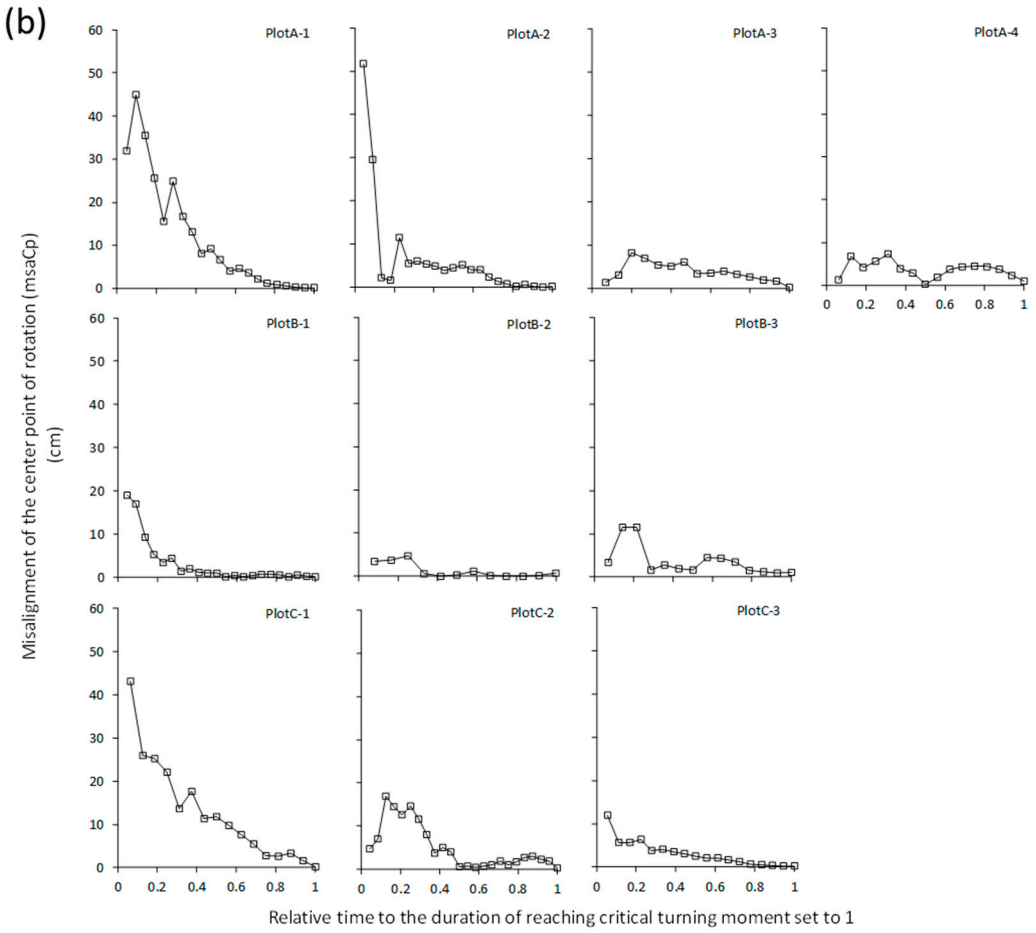

Figure 3. (**a**) Position of the center point of rotation (Cp) in 1 s intervals from the start of the tree-pulling experiment until the critical turning moment was reached in all 10 test trees. The arrows indicate the point at which the critical turning moment was reached. The time of reaching the critical turning moment is indicated in red. (**b**) Misalignment of Cp (msaCp) with relative time to the duration of reaching critical turning moment set to 1 in all 10 test trees.

We found a significantly positive correlation between maximum root depth and Dcp ($r = 0.92$, $p < 0.001$, Figure 4a, Table 2). We observed a significant positive correlation between the Dcp and H, which was stronger than that between the Dcp and H × DBH^2 (H: $r = 0.90$, $p < 0.001$; Figure 4b, Table 2; H × DBH^2: $r = 0.77$, $p < 0.05$; Figure 4c, Table 2). However, we found no significant correlation between the Dcp and DBH ($p = 0.42$). The Dcp was positively, but not significantly, related to the critical turning moment ($r = 0.58$, $p = 0.08$, Figure 4d, Table 2). The above-ground traits that were significantly related to the critical turning moment were the DBH and H × DBH^2 (DBH: $r = 0.77$, $p < 0.05$, H × DBH^2: $r = 0.71$, $p < 0.05$).

The maximum root depth was significantly positively correlated with the critical turning moment ($r = 0.77$, $p < 0.05$, Figure 5a, Table 2). We found significant positive relationships between the maximum root depth and above-ground traits, H or H × DBH^2 (H: $r = 0.82$, $p < 0.01$, Figure 5b, Table 2; H × DBH^2: $r = 0.82$, $p < 0.01$, Figure 5c, Table 2). However, the correlation with the DBH was not significant ($r = 0.50$, $p = 0.14$; Figure 5d, Table 2).

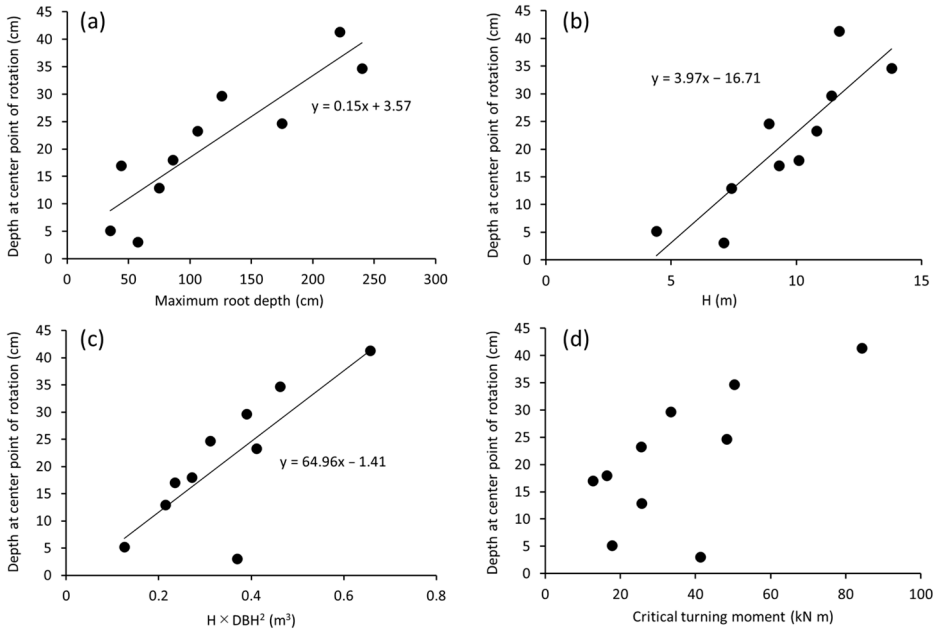

Figure 4. Relationships between (**a**) depth at the center point of rotation (Dcp) and maximum root depth, (**b**) Dcp and H, (**c**) Dcp and H × DBH^2, and (**d**) Dcp and critical turning moment.

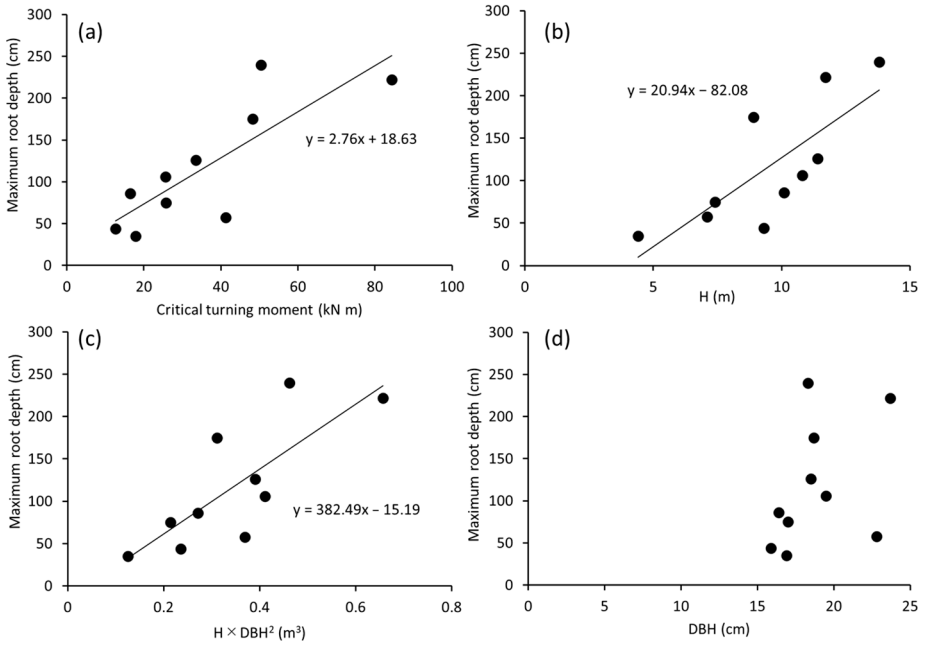

Figure 5. Relationships between (**a**) maximum root depth and critical turning moment, (**b**) maximum root depth and H, (**c**) maximum root depth and H × DBH^2, and (**d**) maximum root depth and DBH.

When we excluded the data for the three trees with plate root systems in plot B, we observed a similar correlation between the Dcp and maximum root depth ($r = 0.93$, $p < 0.01$, Table 2). In contrast, the correlations between the Dcp and H × DBH^2 or critical turning moment were stronger (H × DBH^2: $r = 0.89$, $p < 0.05$; critical turning moment: $r = 0.96$, $p < 0.01$; Table 2).

Table 2. Pearson coefficients for correlations among traits of *Pinus thunbergii* trees.

Parameter	Maximum Root Depth (cm)	H (m)	H × DBH^2 (m^3)	Critical Turning Moment (kN m)
All ten *P. thunbergii* Trees				
Dcp (cm)	0.92 ***	0.90 ***	0.77 *	0.59
Maximum root depth (cm)	–	0.82 **	0.81 **	0.77 *
Seven *P. thunbergii* trees with tap roots excluding three trees with plate root system				
Dcp (cm)	0.93 **	0.75	0.89 *	0.96 **
Maximum root depth (cm)	–	0.64	0.82 *	0.96 **

*** $p < 0.001$, ** $p < 0.01$, * $p < 0.05$.

4. Discussion

4.1. Dcp as an Indicator of Maximum Root Depth

We found that Dcp is a suitable indicator of the maximum root depth of *P. thunbergii* grown in sandy soil in a tree-pulling experiment. Several researchers have measured Dcp [7,17–19,36,38,42]; however, evidence demonstrating its value as a below-ground indicator is lacking. This is the first study in which root depth was measured using actual measurements and compared with the Dcp values. Our results also suggested that measuring Dcp is an appropriate method for easily estimating the maximum root depth without uprooting during tree-pulling experiments as this parameter is usually destructively measured by digging the tree out, which is a laborious process that disturbs the field. The maximum root depth of the trees had a strong positive relationship with the critical turning moment, as shown in the present study (Figure 5a) and previous studies [28,34,50,51]. In particular, the maximum depth of the roots of trees with tap root systems unique to *P. thunbergii* showed a strong positive correlation with the critical turning moment (Table 2). This parameter can be estimated simply by setting up a video camera during tree-pulling experiments and analyzing the video images using relatively easy and non-laborious methods [7,18,36]. Although the Dcp can be estimated using above-ground traits, such as H and H × DBH^2 (Figure 4b,c), this parameter more accurately indicates the maximum root depth (Figure 4a), presumably because it is directly affected by heterogeneous soil conditions [8]. Thus, we propose that the Dcp can be used as an additional parameter with simple measurements when tree-pulling experiments are performed to obtain an important below-ground trait for understanding the critical turning moment.

4.2. Relationship between Cp Displacement and Critical Turning Moment

The Dcp has been defined as the depth of the Cp at the maximum critical turning moment [7,19,36–39]; however, Cp displacement has never been reported in tree-pulling experiments. Our findings demonstrated that the Cp positions mainly fluctuated vertically, not horizontally, until the maximum critical turning moment was reached (Figures 2 and 3). In *P. thunbergii* growing on coastal sandy soil, this indicated that the Cp position must be correctly known to measure the Dcp, which indicates the maximum root depth. In the initial stage of the tree-pulling experiment, the Cp position was relatively shallow and included the above-ground stem, and the Cp positions widely fluctuated compared with those at the later stages (Figure 3). After the initial stage, when the critical turning moment reached the maximum value, Cp was concentrated at a point just below the stem (Figure 3), which is consistent with the Cp positions in *C. japonica* [36] and *C. obtusa* [18]. Similarly, Ennos [52] reported that trees with tap root systems turned and uprooted at a single point immediately below the tree stem. Because the *P. thunbergii* we tested in this study had a tap root system [6], we considered the Cp at the stage when the critical turning moment occurred to have directly converged to a single point under the stem. Hirano et al. [8] showed that *P. thunbergii* trees have distinct tap roots, such as piles, and the root growth depth is more than 200 cm in sandy soil. When lateral forces are applied to a tree, the pile-like taproot is bent by the lateral force [52], which causes uprooting. Our current

findings indicated that when a lateral force is applied to a tree with a deep tap root, the tap root bends at a deeper position, that is, the Cp becomes deeper.

The root system of *P. thunbergii* can adapt to changes from a tap root to a plate root system, depending on environmental conditions, such as groundwater level [8]. In the present study, to examine the correlation between the Dcp and maximum root depth, we separately analyzed three *P. thunbergii* trees with a plate root system in plot B [8], which had high RSP radius/Dcp values of 5.0 (Table 2). The correlations between the Dcp and maximum root depth did not change for any of the ten trees, either those with a plate root system or the seven trees with only a tap root system (Table 2). This suggested that the Dcp acquisition method we used in this study can estimate the maximum root depth even for plate root systems in *P. thunbergii*. However, the correlation between the Dcp and $H \times DBH^2$ or critical turning moment was stronger for the seven *P. thunbergii* trees than for the trees with a plate root system. This result suggested that the Dcp in tap root systems is a more accurate indicator of critical turning moments because the two are more closely related than when trees with plate root systems are included. This result also supports the finding that trees with a heart root system or plate root system show different Cp positions than trees with a tap root system [52,53]. Ennos [52] suggested that in trees with a plate root system, the Cp is positioned near the ground surface; in trees with a heart root system, the Cp is on the opposite side of the tree from the direction of the fall. Further data are needed on the relationship between the maximum root depth and Dcp in trees with different types of root systems, and the location of the Cp to measure the Dcp.

4.3. Relationship between Cp Position and RSP

The position of the Cp in this study supports the findings reported by Karizumi [6], who suggested that the Cp is generally positioned at the bottom of the RSP. Thus, the depth of the RSP is shallower than the maximum root depth [14] because it is assumed to be the depth of the RSP [18,36]. In contrast, the results of our study do not support the position of the Cp at the edge of the RSP on the side in the direction of stem fall, as reported for *P. sitchensis* [9]. The critical turning moment can be divided into two stages [9]. When a tree crown or stem is subjected to lateral force from wind or a tsunami, the tree opposes uprooting, and the first stage is the resistance of the roots and soil. After the soil upwind of the RSP is broken in the first stage, the tree is uprooted because of the weight of the crown and stem. The force exerted to resist uprooting is the second stage [9]. Thus, the contradictory results of the Cp position may be because we measured the critical turning moment and Cp before complete uprooting of the test tree. In other words, we observed the first stage of uprooting, whereas Coutts [9] focused on the second stage of uprooting during the complete felling of a tree. These results suggested that the Cp is directly under the stem during the first stage of uprooting but can move to the edge of the RSP during the second stage. Crook et al. [53] reported that the Cp moved from just below the stem to the edge of the leeward side of the felling direction during the uprooting of *Aglaia affinis* Merr., which has buttress roots. This may also be true for *P. thunbergii* during complete uprooting. Thus, our results suggested that the Dcp should be applied to measure the converged position of the Cp during the first stage of uprooting, which may be an indicator of the maximum root depth.

4.4. Relationship between Soil Type and Cp Displacement

In this study, we focused on the Cp displacement in *P. thunbergii* in sandy coastal soil. Coastal forests have been cultivated in many coastal areas of Japan over the past several hundred years to protect against damage caused by strong sand-laden sea winds, tides, and tsunamis [1–4]. *P. thunbergii* is the most important tree species in these forests owing to its high tolerance to salt and poor nutrient availability [1–4]. During the Great East Japan Earthquake, many *P. thunbergii* were severely damaged by the following tsunami, so clarifying the relationship between the maximum root depth and uprooting of *P. thunbergii* would be useful [5]. Fourcaud et al. [40] simulated the Cp position using the finite element

method when a tree with a herringbone-like root system overturned, and compared the results between clay and sandy soils. Their findings suggested that during overturning, the Cp moved more leeward in sandy soil than in clay soil, and the Dcp was shallow in a model root system without tap roots. In this study, the horizontal Cp displacements occurred in the pull direction (Figure 3). In plot B, *P. thunbergii* developed horizontal roots without tap roots, and the vertical Cp displacements were shallower than those in plots A and C (Figure 3, Table 1). These results are consistent with those reported by Fourcaud et al. [40]. Fourcaud et al. [40] also reported that the effect of tap roots on tree resistance to overturning was higher in sandy than in clayey soils. Therefore, the estimation of the maximum root depth using the Dcp to examine the anchorage of coastal *P. thunbergii* is justifiable. However, Fourcaud et al. [40] reported that the location and displacement of the Cp in sandy soils differ from those in clay soils. In addition, clay and sandy soils have different moisture environments around the roots [24], which can induce different relationships between the physical traits of roots and soils. Therefore, examining the relationship between the maximum root depth and Dcp of *P. thunbergii* and the position of the Cp is necessary, which indicates the maximum root depth in other soil types.

Knowing the maximum root depth of *P. thunbergii* in coastal forests can provide insights into the resistance of *P. thunbergii* to tsunamis. Whether coastal forest areas will be prone to collapse or resistant to future tsunamis can be predicted. Fraser [54] suggested that drainage induced deeper rooting in *P. sitchensis,* which increased the resistance to uprooting by 25%. Management practices such as drainage and embankments, which are necessary to ensure the availability of sufficient space for root growth in the depth direction [49], can be incorporated to create a coastal forest with higher tree stability.

5. Conclusions

In this study, we revealed that the maximum root depth of *P. thunbergii,* which is a crucial below-ground parameter for the critical turning moment, could be estimated from the Dcp during a tree-pulling experiment. We determined the vertical and horizontal displacements of the Cp position, and proposed the measurement position of the Dcp. Measurements of indicators of below-ground tree parts and relevant data collection allowed us to comprehensively understand the relationship between tree stability and root system structure. The root system structure of *P. thunbergii* is closely related to variations in the critical turning moment. However, the Dcp must still be measured for destructive tree-pulling experiments. Recently, nondestructive geophysical surveys on soil surfaces using ground penetrating radar have been used to estimate the position and diameter of tree roots as point datasets [31,55]. When an algorithm to reconstruct the point data of root position and size into the whole root system structure is established in a specific tree species [56], the maximum root depth can be nondestructively estimated.

Further studies on the establishment of indicators for the highly accurate estimation of the maximum root depth and horizontal spreading of root systems are needed to improve the mitigation of *P. thunbergii* damage caused by natural disasters such as strong winds, heavy rainfall, and tsunamis.

Supplementary Materials: The following supporting information can be downloaded at https://www.mdpi.com/article/10.3390/f13091506/s1. Figure S1: Location of experimental plots A–C in a coastal *Pinus thunbergii* forest.; Figure S2: Video-shooting method used to measure depth at center point of rotation (Dcp) in *P. thunbergii* trees in tree-pulling experiment.; Figure S3. Example of change in applied force with the pulling time in a *P. thunbergii* tree during the pulling experiment (ex. plotA-1).; Table S1: The depth of the water table belowground level, soil water content, and characteristics of *Pinus thunbergii* trees at Plot A, B and C (min–max values or mean values ± SE).

Author Contributions: C.T. planned and performed the experiment, conducted data analyses, wrote the paper, and prepared the manuscript for submission; K.Y. planned and performed the experiment and conducted data analyses; H.I. planned and performed the experiment and conducted data analyses; T.T. performed the experiment and conducted data analyses; M.O. conducted data analyses;

Y.H. planned and performed the experiment, conducted data analyses, and wrote and edited the manuscript. All authors have read and agreed to the published version of the manuscript.

Funding: This study was partially supported by JSPS KAKENHI (grant nos. JP25252027 and 20H03028), and the 28th and 29th Botanical Research Grants from the ICHIMURA Foundation for New Technology.

Data Availability Statement: Not applicable.

Acknowledgments: We thank H. Kitahara (Shinshu University) for their valuable suggestions regarding the method for measuring the center point of rotation. We also thank R. Doi, R. Wada (Nagoya University), K. Okuda, K. Kujihashi (University of Hyogo), M. Dannoura, J. An, R. Nakahata (Kyoto University), S. Ohashi (Manbokuen), and M. Harano (Aichi Branch, Japan Tree Doctor Association) for their invaluable field assistance. We thank J. Tanaka (Japan Conservation Engineers & Co., Ltd.), N. Yamashita, H. Nakashima (Aichi Prefectural Forestry Technology Center), and the Aichi Prefecture Fish Farming Center for their permission to conduct this experiment at their study site.

Conflicts of Interest: The authors declare that they have no conflict of interests.

References

1. Murai, H.; Ishikawa, M.; Endo, J.; Tadaki, Y. *The Coastal Forest in Japan*; Soft Science Inc.: Tokyo, Japan, 1992; p. 513. (In Japanese)
2. Zhu, J.; Matsuzaki, T.; Sakioka, K. Windspeeds within a single crown of Japanese black pine (*Pinus thunbergii* Parl.). *For. Ecol. Manag.* **2000**, *135*, 19–31. [CrossRef]
3. Konta, F. The present conditions and functions of the coastal forests in Japan. *J. Jpn. Soc. Coast. For.* **2001**, *1*, 1–4. (In Japanese with English summary)
4. Ogawa, M. Microbial flora in *Pinus thunbergii* forest of coastal sand dune. *Bull. For. For. Prod. Res. Inst.* **1979**, *305*, 107–124. (In Japanese with English summary)
5. Forestry and Forest Products Research Institute. *Regeneration of Coastal Forests Affected by Tsunami*; Forestry and Forest Products Research Institute: Tsukuba, Japan, 2012; pp. 1–24.
6. Karizumi, N. *The Illustrations of Tree Roots*; Seibundoshinko-sya: Tokyo, Japan, 1979; p. 1121. (In Japanese)
7. Todo, C.; Tokoro, C.; Yamase, K.; Tanikawa, T.; Ohashi, M.; Ikeno, H.; Dannoura, M.; Miyatani, K.; Doi, R.; Hirano, Y. Stability of *Pinus thunbergii* between Two Contrasting Stands at Differing Distances from the Coastline. *For. Ecol. Manag.* **2019**, *431*, 44–53. [CrossRef]
8. Hirano, Y.; Todo, C.; Yamase, K.; Tanikawa, T.; Dannoura, M.; Ohashi, M.; Doi, R.; Wada, R.; Ikeno, H. Quantification of the Contrasting Root Systems of *Pinus thunbergii* in Soils with Different Groundwater Levels in a Coastal Forest in Japan. *Plant Soil.* **2018**, *426*, 327–337. [CrossRef]
9. Coutts, M.P. Components of Tree Stability in Sitka Spruce on Peaty Gley Soil. *Forestry* **1986**, *59*, 173–197. [CrossRef]
10. Ray, D.; Nicoll, B.C. The Effect of Soil Water-Table Depth on Root-Plate Development and Stability of Sitka Spruce. *Forestry* **1998**, *71*, 169–182. [CrossRef]
11. Moore, J.R. Differences in Maximum Resistive Bending Moments of *Pinus radiata* Trees Grown on a Range of Soil Types. *For. Ecol. Manag.* **2000**, *135*, 63–71. [CrossRef]
12. Peltola, H.; Kellomäki, S.; Hassinen, A.; Granander, M. Mechanical Stability of Scots Pine, Norway Spruce and Birch: An Analysis of Tree-Pulling Experiments in Finland. *For. Ecol. Manag.* **2000**, *135*, 143–153. [CrossRef]
13. Cucchi, V.; Meredieu, C.; Stokes, A.; Berthier, S.; Bert, D.; Najar, M.; Denis, A.; Lastennet, R. Root Anchorage of Inner and Edge Trees in Stands of Maritime Pine (*Pinus pinaster* Ait.) Growing in Different Podzolic Soil Conditions. *Trees* **2004**, *18*, 460–466. [CrossRef]
14. Nicoll, B.C.; Achim, A.; Mochan, S.; Gardiner, B.A. Does Steep Terrain Influence Tree Stability? A Field Investigation. *Can. J. For. Res.* **2005**, *35*, 2360–2367. [CrossRef]
15. Tanaka, N. Effectiveness and Limitations of Coastal Forest in Large Tsunami: Conditions of Japanese Pine Trees on Coastal Sand Dunes in Tsunami Caused by Great East Japan Earthquake. *J. Jpn. Soc. Civ. Eng. Ser. B1* **2012**, *68*, II_7–II_15. [CrossRef]
16. Nicoll, B.C.; Gardiner, B.A.; Rayner, B.; Peace, A.J. Anchorage of Coniferous Trees in Relation to Species, Soil Type, and Rooting Depth. *Can. J. For. Res.* **2006**, *36*, 1871–1883. [CrossRef]
17. Todo, C.; Yamase, K.; Tanikawa, T.; Ohashi, M.; Ikeno, H.; Dannoura, M.; Hirano, Y. Effect of Thinning on the Critical Turning Moment of Sugi (*Cryptomeria japonica* (L. f.) D. Don). *J. Jpn. Soc. Reveget Tec.* **2015**, *41*, 308–314. (In Japanese with English summary) [CrossRef]
18. Nonoda, T.; Hayashi, S.; Kawabe, H.; Honda, K.; Koyabu, K. The Mechanism of the Tree-Uprooting Occurred by Pulling Down a Tree. *J. Jpn. For. Soc.* **1996**, *78*, 390–397. (In Japanese with English summary) [CrossRef]
19. Okada, Y. Measuring the Critical Turning Moment of the Japanese Cedar (*Cryptomeria japonica*) in situ. *J. For. Res.* **2019**, *24*, 168–177. [CrossRef]
20. Lundström, T.; Jonas, T.; Stöckli, V.; Ammann, W. Anchorage of Mature Conifers: Resistive Turning Moment, Root–Soil Plate Geometry and Root Growth Orientation. *Tree Physiol.* **2007**, *27*, 1217–1227. [CrossRef]

21. Hale, S.E.; Gardiner, B.A.; Wellpott, A.; Nicoll, B.C.; Achim, A. Wind Loading of Trees: Influence of Tree Size and Competition. *Eur. J. For. Res.* **2012**, *131*, 203–217. [CrossRef]
22. Tanikawa, T.; Ikeno, H.; Todo, C.; Yamase, K.; Ohashi, M.; Okamoto, T.; Mizoguchi, T.; Nakao, K.; Kaneko, S.; Torii, A.; et al. A Quantitative Evaluation of Soil Mass Held by Tree Roots. *Trees* **2021**, *35*, 527–541. [CrossRef]
23. Bischetti, G.B.; Chiaradia, E.A.; Simonato, T.; Speziali, B.; Vitali, B.; Vullo, P.; Zocco, A. Root Strength and Root Area Ratio of Forest Species in Lombardy (Northern Italy). *Plant Soil* **2005**, *278*, 11–22. [CrossRef]
24. Giambastiani, Y.; Preti, F.; Errico, A.; Sani, L. On the Tree Stability: Pulling Tests and Modelling to Assess the Root Anchorage. *Procedia Environ. Sci. Eng. Manag.* **2017**, *4*, 207–218.
25. Giambastiani, Y.; Guastini, E.; Preti, F.; Censini, G. Laboratory Tests About Resistivity Variation in Soil, in Connection with Root Presence. *Geophys. Res.* **2021**, *22*, 46–61. [CrossRef]
26. Giambastiani, Y.; Errico, A.; Preti, F.; Guastini, E.; Censini, G. Indirect Root Distribution Characterization Using Electrical Resistivity Tomography in Different Soil Conditions. *Urban For. Urban Green.* **2022**, *67*, 127442. [CrossRef]
27. Nicoll, B.C.; Gardiner, B.A.; Peace, A.J. Improvements in Anchorage Provided by the Acclimation of Forest Trees to Wind Stress. *Forestry* **2008**, *81*, 389–398. [CrossRef]
28. Yang, M.; Défossez, P.; Danjon, F.; Dupont, S.; Fourcaud, T. Which Root Architectural Elements Contribute the Best to Anchorage of *Pinus* species? Insights From In Silico Experiments. *Plant Soil* **2017**, *411*, 275–291. [CrossRef]
29. Preti, F. Forest Protection and Protection Forest: Tree Root Degradation Over Hydrological Shallow Landslides Triggering. *Ecol. Eng.* **2013**, *61*, 633–645. [CrossRef]
30. Giadrossich, F.; Schwarz, M.; Marden, M.; Marrosu, R.; Phillips, C. Minimum Representative Root Distribution Sampling for Calculating Slope Stability in *Pinus radiata* D.Don Plantations in New Zealand. *N. Z. J. For. Sci.* **2020**, *50*, 5. [CrossRef]
31. Yamase, K.; Tanikawa, T.; Dannoura, M.; Ohashi, M.; Todo, C.; Ikeno, H.; Aono, K.; Hirano, Y. Ground-penetrating radar estimates of tree root diameter and distribution under field conditions. *Trees* **2018**, *32*, 1657–1668. [CrossRef]
32. Danjon, F.; Stokes, A.; Bakker, M.R. Root Systems of Woody Plants. In *Plant Roots*; The Hidden Half; CRC Press: Boca Raton, FL, USA, 2013; p. 848.
33. Kokutse, N.K.; Temgoua, A.G.T.; Kavazović, Z. Slope Stability and Vegetation: Conceptual and Numerical Investigation of Mechanical Effects. *Ecol. Eng.* **2016**, *86*, 146–153. [CrossRef]
34. Yang, M.; Défossez, P.; Danjon, F.; Fourcaud, T. Analyzing Key Factors of Roots and Soil Contributing to Tree Anchorage of *Pinus* species. *Trees* **2018**, *32*, 703–712. [CrossRef]
35. Dupuy, L.; Fourcaud, T.; Stokes, A. A Numerical Investigation into Factors Affecting the Anchorage of Roots in Tension. *Eur. J. Soil Sci.* **2005**, *56*, 319–327. [CrossRef]
36. Morioka, N. Strength of Standing Trees for Logging Cable Support (II) Method to Find the Center of Moment of Force That Makes Tree Incline. *J. Jpn. For. Soc.* **1983**, *65*, 342–346. (In Japanese) [CrossRef]
37. Morioka, N. Strength of Standing Trees for Logging Cable Support (III) on the Relation Between Moment of a Lateral Force and Stem Inclination. *J. Jpn. For. Soc.* **1984**, *66*, 160–163. (In Japanese) [CrossRef]
38. Shimada, H.; Nonoda, T. Critical Turning Moment of sugi (*Cryptomeria japonica* (L.f.) D. Don) and Hinoki (*Chamaecyparis obtusa* (Siebold et Zucc.) Endl). In central Mie Prefecture. *J. Jpn. Soc. Reveget. Technol.* **2017**, *43*, 138–143. (In Japanese with English summary) [CrossRef]
39. Kamimura, K.; Kitagawa, K.; Saito, S.; Mizunaga, H. Root Anchorage of Hinoki (*Chamaecyparis obtuse* (Sieb. et Zucc.) Endl.) Under the Combined Loading of Wind and Rapidly Supplied Water on Soil: Analyses Based on Tree-Pulling Experiments. *Eur. J. For. Res.* **2012**, *131*, 219–227. [CrossRef]
40. Fourcaud, T.; Ji, J.N.; Zhang, Z.Q.; Stokes, A. Understanding the Impact of Root Morphology on Overturning Mechanisms: A Modelling Approach. *Ann. Bot.* **2008**, *101*, 1267–1280. [CrossRef]
41. Tanaka, J.; Nakazawa, H.; Satou, T. Case Study of Root Systems Growth of *Pinus thunbergii* Parlatore and Groundwater Level in the Nishinohama Coastal Forest, Tahara City, Aichi Prefecture. *J. Jpn. Soc. Reveget Tec.* **2017**, *43*, 298–301. (In Japanese) [CrossRef]
42. Todo, C.; Ikeno, H.; Yamase, K.; Tanikawa, T.; Ohashi, M.; Dannoura, M.; Kimura, T.; Hirano, Y. Reconstruction of Conifer Root Systems Mapped with Point Cloud Data Obtained by 3D Laser Scanning Compared with Manual Measurement. *Forests* **2021**, *12*, 1117. [CrossRef]
43. Tahara City. Damage Investigation for Nankai Megathrust Earthquake in Tahara City. 2015, p. 26. Available online: http://www.city.tahara.aichi.jp/_res/projects/default_project/_page_/001/001/437/mayor/newsconference/pdf/1506/1506_1-1nankaitorafu-higaisoutei.pdf (accessed on 30 August 2022).
44. Sakamoto, T.; Noguchi, H.; Gotoh, Y.; Suzuki, S.; Shimada, K. Management of Japanese Black Pine (*Pinus thunbergii*) Seedlings Caused by Natural Regeneration. *J. Jpn. Soc. Coast. For.* **2013**, *12*, 29–34. (In Japanese with English summary)
45. Suzuki, Y.; Yoshizaki, S. On the natural generation process of Black pine forests at Nishinohama coastal forest of Tahara City, Aichi Pref., Japan. *J. Jpn. Soc. Reveget Tech.* **2016**, *42*, 256–359. (In Japanese) [CrossRef]
46. FAO-UNESCO. Soil Map of the World. Revised Legend. Reprinted with Corrections. In *World Soil Resources Report 60*; Food and Agriculture Organization: Rome, Italy, 1990; p. 119.
47. Japan Meteorological Agency. 2019. Available online: http://www.data.jma.go.jp/obd/stats/etrn/ (accessed on 12 August 2019).
48. Schneider, C.A.; Rasband, W.S.; Eliceiri, K.W. NIH Image to ImageJ: 25 Years of Image Analysis. *Nat. Methods.* **2012**, *9*, 671–675. [CrossRef] [PubMed]

49. R Core Team. *R: A Language and Environment for Statistical Computing*; R Foundation for Statistical Computing: Vienna, Austria, 2020; Available online: https://www.R-project.org/ (accessed on 12 July 2020).
50. Danjon, F.; Barker, D.H.; Drexhage, M.; Stokes, A. Using Three-Dimensional Plant Root Architecture in Models of Shallow-Slope Stability. *Ann. Bot.* **2008**, *101*, 1281–1293. [CrossRef] [PubMed]
51. Danjon, F.; Fourcaud, T.; Bert, D. Root Architecture and Wind-Firmness of Mature *Pinus pinaster*. *New Phytol.* **2005**, *168*, 387–400. [CrossRef]
52. Ennos, A.R. The Mechanics of Root Anchorage. *Adv. Bot. Res.* **2000**, *33*, 133–157. [CrossRef]
53. Crook, M.J.; Ennos, A.R.; Banks, J.R. The Function of Buttress Roots: A Comparative Study of the Anchorage Systems of Buttressed (*Aglaia* and *Nephelium ramboutan* species) and Non-buttressed (*Mallotus wrayi*) Tropical Trees. *J. Exp. Bot.* **1997**, *48*, 1703–1716. [CrossRef]
54. Fraser, A.I. The soil and roots as factors in tree stability. *Forestry* **1962**, *34*, 117–127. [CrossRef]
55. Hirano, Y.; Yamamoto, R.; Dannoura, M.; Aono, K.; Igarashi, T.; Ishii, M.; Yamase, K.; Makita, N.; Kanazawa, Y. Detection Frequency of *Pinus thunbergii* Roots by Ground-Penetrating Radar Is Related to Root Biomass. *Plant Soil* **2012**, *360*, 363–373. [CrossRef]
56. Ohashi, M.; Ikeno, H.; Sekihara, K.; Tanikawa, T.; Dannoura, M.; Yamase, K.; Todo, C.; Tomita, T.; Hirano, Y. Reconstruction of Root Systems in *Cryptomeria japonica* Using Root Point Coordinates and Diameters. *Planta* **2019**, *249*, 445–455. [CrossRef]